

NMR Study on the Photoresponsive DNA Tethering an Azobenzene. Assignment of the Absolute Configuration of Two Diastereomers and Structure Determination of Their Duplexes in the *trans*-Form

Xingguo Liang,[†] Hiroyuki Asanuma,^{*,†, ‡} Hiromu Kashida,[†] Akitsugu Takasu,^{§,||,⊥} Taiichi Sakamoto,[§] Gota Kawai,[§] and Makoto Komiyama^{*,†}

Contribution from the Research Center for Advanced Science and Technology, The University of Tokyo, 4-6-1 Komaba, Meguro-ku, Tokyo 153-8904, Japan; PRESTO, Japan Science and Technology Corporation (JST), Kawaguchi 332-0012 Japan; Department of Industrial Chemistry, Chiba Institute of Technology, 2-17-1 Tsudanuma, Narashino-shi, Chiba 275-0016, Japan; and Department of Chemistry and Biotechnology, Graduate School of Engineering, University of Tokyo, 7-3-1 Hongo, Bunkyo-ku, Tokyo 113-8656, Japan

Received July 14, 2003; E-mail: asanuma@mkomi.rcast.u-tokyo.ac.jp; komiyama@mkomi.rcast.u-tokyo.ac.jp

Abstract: Two diastereomers of a photoresponsive oligodeoxyribonucleotide tethering a *trans*-azobenzene, based on the chirality of the central carbon of a diol linker, were separated by reversed-phase HPLC. On the basis of 2D NMR analysis, absolute configurations of the diastereomers α and β (tentatively designated from differences in their retention time) were determined as *R*- and *S*-forms, respectively. For both diastereomers, their NMR-determined duplex structure showed that *trans*-azobenzene intercalates between base pairs, because distinct NOEs were observed between the protons of azobenzene and those of the adjacent base pairs, such as with the imino protons and methyl protons of thymine. The melting temperatures of both duplexes were higher than that of the corresponding native duplex, which contained no azobenzene residue, due to the intercalated *trans*-azobenzene stabilizing the duplex by a stacking interaction. Between these two diastereomers, differences in T_m were also found: the melting temperature of the *R*-form duplex (α -isomer) was higher than that of the *S*-form (β -isomer). On the basis of the NMR-determined structure, this difference was attributed to the fact that the *S*-form (β isomer) causes more stress forming the duplex than does the *R*-form (α isomer) due to disturbances of the right-hand helix.

Introduction

Several strategies have been proposed for the photoregulation of DNA function, such as the introduction of photoresponsive moieties into proteins to photoregulate their binding force to DNA or RNA.¹ Azobenzene, a commonly used photoresponsive switch, has been tethered to some polyamides, which can bind to the minor groove of a DNA duplex.² In our previous studies, azobenzene was introduced into a DNA side chain, and its duplex formation was regulated by photostimuli.^{3a,b} Upon irradiation with either UV or visible light, the duplex-forming

activities of the modified oligonucleotides were reversibly controlled due to *cis*–*trans* photoisomerization of the azobenzene residue. Through use of these azobenzene-modified DNAs, DNA polymerase^{3c} and RNA polymerase^{3d} reactions were also successfully photoregulated.

To tether an azobenzene to DNA, we used 2,2-bis(hydroxymethyl)propionic acid (see Scheme 1) as a linker. Because this compound is prochiral, two diastereomers of the modified DNAs were obtained as a mixture which could be separated from each other by reversed-phase HPLC.⁴ Interestingly, a large difference in the photoregulation ability of the two diastereomers was found:^{3a,b,4} the melting temperature of the *trans*-form of one diastereomer (α -isomer) was higher than that of the other diastereomer (β -isomer), whereas the T_m of the *cis*-form of the α -isomer was lower than that of the β -isomer. As a result, the α -isomer exhibited a larger T_m change for *trans*–*cis* isomerization than did the β -isomer. This result means that the chirality of the linker that tethers nonnatural functional molecules is important in the design of modified DNA. However, the absolute configuration of these diastereomers, which should be significant

(4) Asanuma, H.; Ito, T.; Komiyama, M. *Tetrahedron Lett.* **1998**, *39*, 9015–9018.

[†] RCAST, The University of Tokyo.

[‡] JST.

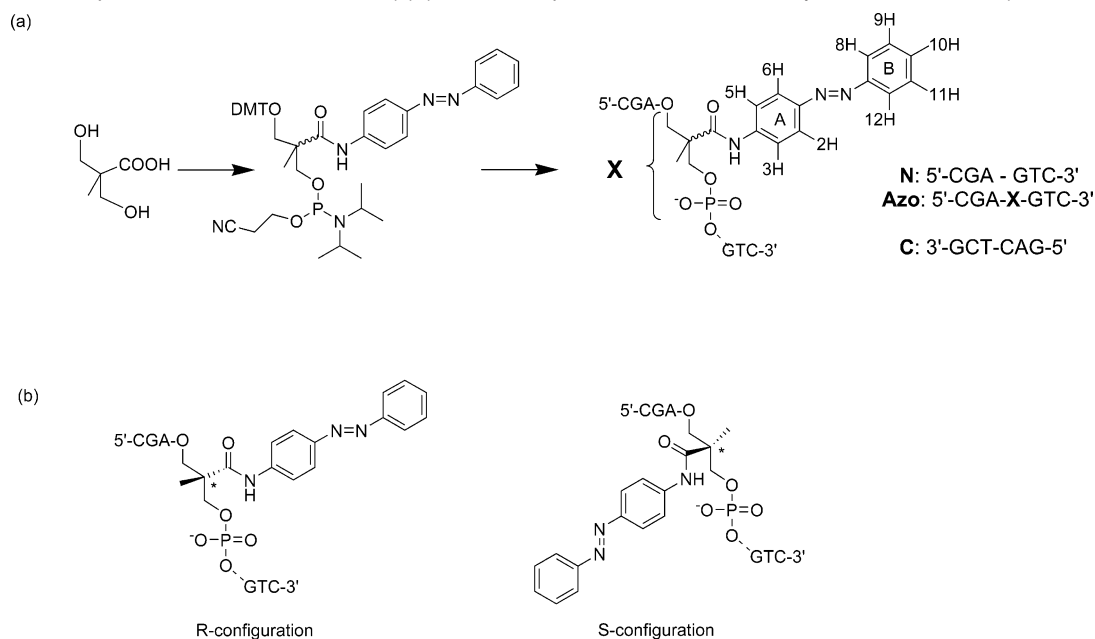
[§] Chiba Institute of Technology.

^{||} Department of Chemistry and Biotechnology, The University of Tokyo.

[⊥] Present address: Protein Research Group, RIKEN Genomic Sciences Center (GSC), 1-7-22 Suehiro-cho, Tsurumi-ku, Yokohama, Kanagawa, 230-0045 Japan.

(1) Willner, I.; Rubin, S. *Angew. Chem., Int. Ed. Engl.* **1996**, *35*, 367.
(2) Hoshaka, T.; Kawashima, K.; Sisido, M. *J. Am. Chem. Soc.* **1994**, *116*, 413.
(3) (a) Asanuma, H.; Ito, T.; Yoshida, T.; Liang X. G.; Komiyama, M. *Angew. Chem., Int. Ed.* **1999**, *38*, 2393–2395. (b) Asanuma, H.; Liang X. G.; Yoshida, T.; Komiyama, M. *ChemBioChem.* **2000**, *2*, 39–44. (c) Yamazawa, A.; Liang, X. G.; Asanuma, H.; Komiyama, M. *Angew. Chem., Int. Ed.* **2000**, *39*, 2356–2358. (d) Asanuma, H.; Tamaru, D.; Yamazawa, A.; Liu, M. Z.; Komiyama, M. *ChemBioChem.* **2002**, *3*, 786–89.

Scheme 1. Introduction of an Azobenzene Moiety Using Prochiral 2,2-Bis(hydroxymethyl)propionic Acid as a Linker (a), and the Absolute Configuration with Respect to the Asterisked Carbon (b) (the DNA Sequences Used in This Study Are Also Presented)



for clarifying the mechanism of photoregulation of DNA function, has not yet been determined.

In the present paper, we focus on the duplex tethering a *trans*-azobenzene using a prochiral linker and determine the absolute configuration of each diastereomer, as well as the structure of the duplex by NMR measurements. On the basis of the structure analysis, the effect of the chirality of the linker on the duplex-forming stability using *trans*-azobenzene is also discussed.

Results and Discussion

1. NMR Analysis of the Duplex Composed of Azobenzene-Tethered DNA and Its Complementary Strand.

1.1. Imino Protons in the Base Pair. The azobenzene moiety (X residue) was introduced into the middle position of the 6-mer DNA using a prochiral diol linker (Scheme 1a). Two diastereomers of the modified DNA (**Azo:** 5'-CGAXGTC-3'), based on the chiral carbon of the linker tethering an azobenzene, were separated by reversed-phase HPLC.^{3a,b,4} Thereafter, the diastereomer with the shorter retention time was designated as α (**Azo- α**) and the other as β (**Azo- β**). As a counterpart, DNA **C** composed of six natural nucleotides was used.⁵ **Azo- α /C** and **Azo- β /C** were thus 7-mer/6-mer nonsymmetrical duplexes involving *trans*-azobenzene. For both of the diastereomers, as well as the native DNA **N**, the 1D and 2D NMR spectra were measured both in H₂O (H₂O/D₂O = 9:1) and in D₂O to enable structural information to be obtained regarding their duplexes with **C**. Combined with the NOESY, DQF-COSY, and TOCSY spectra in D₂O, most of the signals of the duplex were assigned. In Figure 1, 1D and NOESY spectra measured in H₂O at the region of the imino-protons (11–14 ppm) are shown for the duplexes of **Azo- α /C**, **Azo- β /C**, and **N/C**. Almost the same spectra were observed for the α and β diastereomers in this region (compare Figure 1a with 1b): there were six signals corresponding to the six hydrogen-bonded base pairs, which can be assigned on the basis of NOESY spectra. The signals of

the base pairs adjacent to the azobenzene moiety (designated as T¹⁰ and G⁴ in Figure 1) remained sharp regardless of the additional X residue. Furthermore, a large upfield shift as compared to the **N/C** duplex was observed for these T¹⁰ and G⁴ signals in the **Azo/C** duplex (about 1 ppm), indicating that the ring current of azobenzene affects the chemical shift of these protons. It should be noted that the NOE between T¹⁰ and G⁴ of the **Azo/C** duplex either in the α or in the β diastereomers was not observed, whereas a distinct NOE appeared between them in the **N/C** duplex (Figure 1c). This fact indicates that two base pairs are separated by the intercalated azobenzene.⁶

1.2. Direct Evidence for Intercalation of *trans*-Azobenzene.

To confirm the intercalation of azobenzene, NOEs between the aromatic protons of the *trans*-azobenzene residue and the imino protons of the adjacent base pairs were measured (Figure 2). For diastereomer α , the NOE signals between G⁴ (as well as T¹⁰) and 8H (or 12H) protons of azobenzene were strong, indicating that the distance between these protons is short.⁷ These results demonstrate that the benzene ring B (far from the backbone) in the azobenzene is located between the base pairs T¹⁰-A³ and G⁴-C⁹. On the other hand, the benzene ring A (connected directly to the backbone) is relatively far from them. These NOE data indicate that *trans*-azobenzene is located between two base pairs of the DNA duplex. Similar results have been observed for diastereomer β (Figure 2b): strong NOEs between G⁴, T¹⁰, and 8H (or 12H) were observed. These NOEs show that the *trans*-azobenzene of diastereomer β also intercalates between base pairs. Intercalation of the *trans*-azobenzene was also confirmed from the NOEs between all of the protons on the benzene ring B of the *trans*-azobenzene (from 8H to

(5) By this combination, X residue is additionally incorporated into the natural full-matched 6-mer duplex.

(6) Although 1D and 2D NMR spectra of the duplex containing *cis*-azobenzene were also measured, the spectra were too complicated to be solved because of the thermal instability of the duplex of the *cis*-form and the influence of the much more stable *trans*-form duplex (only 70% is isomerized to the *cis*-form under the conditions employed).

(7) Proton signals of the pairs of 2 and 6, 3 and 5, 8 and 12, and 9 and 11 on the azobenzene were equivalent to each other even in the duplex.

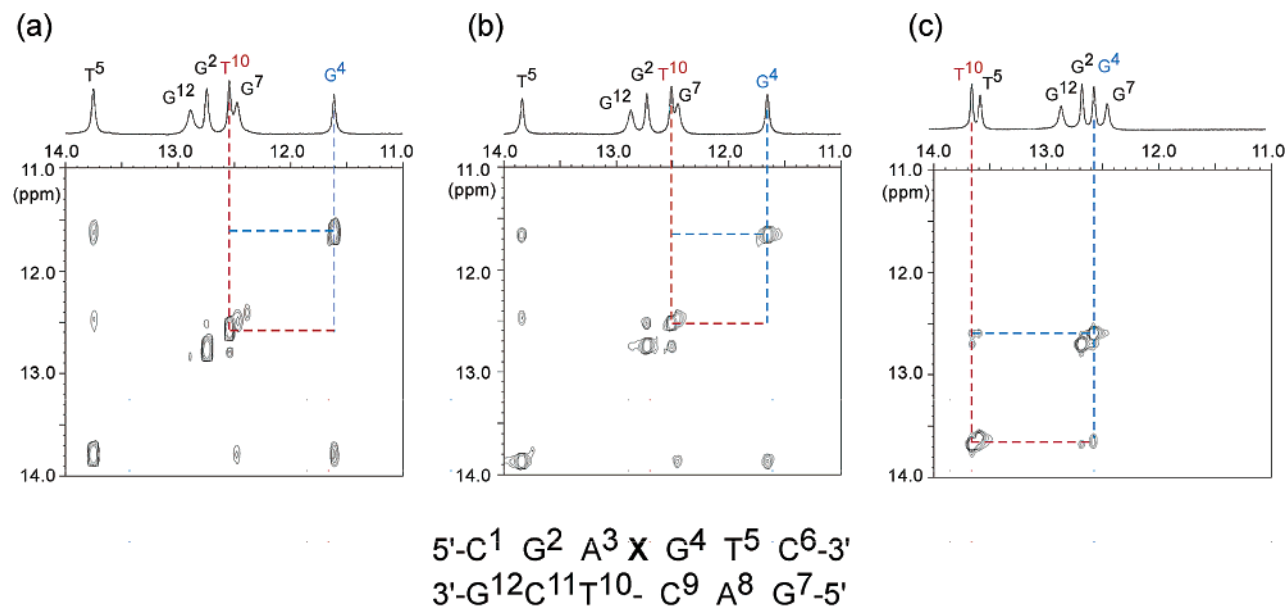


Figure 1. 2D NOESY spectra (imino proton region) of the duplexes (a) *Azo-α/C*, (b) *Azo-β/C*, and (c) *N/C* in H₂O/D₂O (9/1) at 280 K (mixing time = 150 ms), pH 7.0 (10 mM phosphate buffer) in the presence of 0.2 M NaCl. Imino proton assignments are denoted on the projected 1D spectrum with the residue number shown in the bottom.

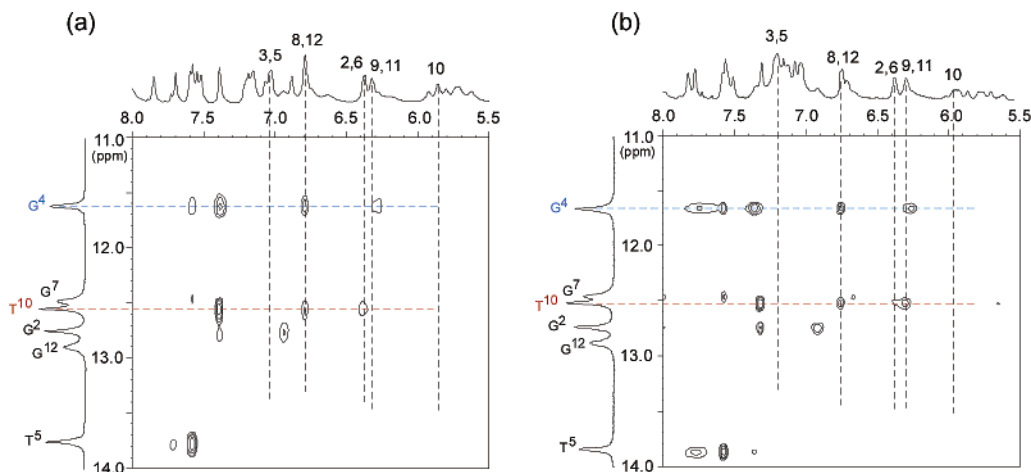


Figure 2. 2D NOESY spectra (mixing time = 150 ms) between the aromatic proton signal (5.5–8 ppm) and imino proton signal regions (11–14 ppm) for (a) *Azo-α/C* and (b) *Azo-β/C* in H₂O/D₂O (9/1) at 280 K, pH 7.0 (10 mM phosphate buffer) in the presence of 0.2 M NaCl. Assignments of azobenzene protons are denoted on the projected 1D spectra (F2 axis) with numbers designated in Scheme 1a.

12H) and CH₃ on T¹⁰, which were observed for both the *Azo-α/C* and the *Azo-β/C* duplexes.⁸

1.3. Determination of the Absolute Configuration (*R* or *S*) of Azobenzene-Modified DNA. According to the above analysis, the azobenzene moiety intercalates between base pairs for both the *α*- and the *β*-isomers. When the modified DNA (*Azo-α* or *Azo-β*) takes the *R*-configuration with the azobenzene moiety intercalated, the methyl group in the X residues (X–CH₃) should protrude to the major groove, and the X–CH₃ and 8H of the adenine base (A³–8H), which are adjacent to this azobenzene residue, should become close enough to provide a distinct NOE between these protons (see Figure 3a). On the other hand, if *Azo* takes the *S*-configuration, the X–CH₃ would protrude to the minor groove and the distance between X–CH₃ and A³–8H would be relatively long, giving rise to an extremely weak NOE (see Figure 3b). Therefore, the absolute configuration

of each diastereomer can be determined on the basis of the intensity of the NOE between X–CH₃ and A³–8H.

The NOESY spectra for both diastereomers in the region of 0–2.0 ppm (F1 axis) and 7.0–8.5 ppm (F2 axis) are shown in Figure 4. For diastereomer *α* (Figure 4a), a relatively strong NOE between methyl protons of X–CH₃ and A³–8H was detected. However, for diastereomer *β*, the corresponding NOE was hardly observed (Figure 4b). Thus, it is concluded that *Azo-α* (with a shorter HPLC retention time) takes the *R*-configuration, whereas *Azo-β* takes the *S*-configuration (see Scheme 1b).

2. Structure Determination of the Duplex Tethering a *trans*-Azobenzene Moiety. From the NOESY, TOCSY, and DQF-COSY spectra in D₂O, all chemical shifts of nonexchangeable protons in the duplex (except 5'H and 5''H of ribose and the methylene (CH₂) protons in the linker) were assigned using the established techniques. The distances between all of the atoms in the duplex were calculated according to the strength

(8) All of the NOEs concerning the azobenzene are displayed with lines on the structure in Supporting Information Figure 1.

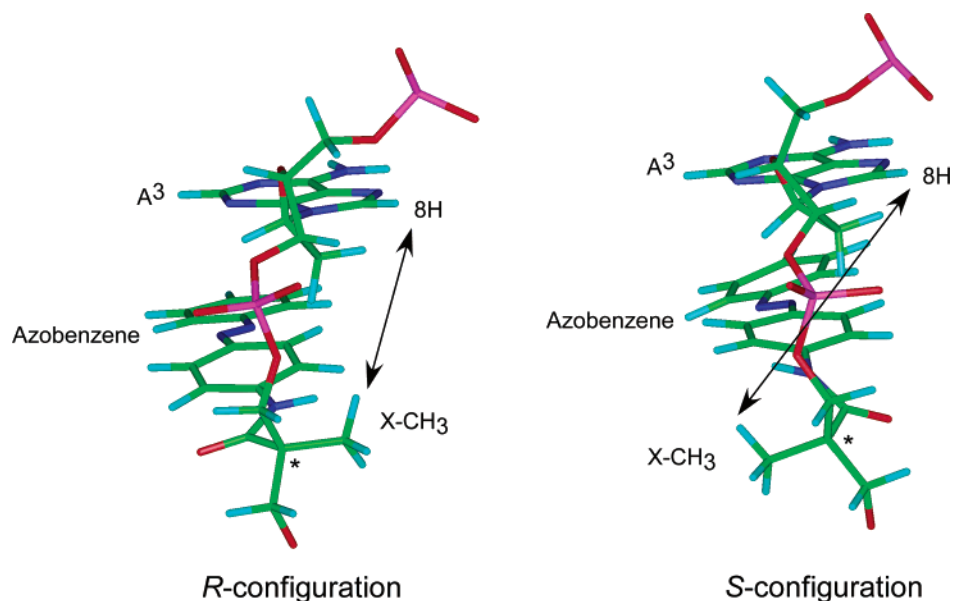


Figure 3. Correlation between the absolute configuration of the central carbon (asterisked) of the linker and positions of X-CH₃ and A³-8H, which become closer to each other when the diastereomer takes the *R*-configuration.

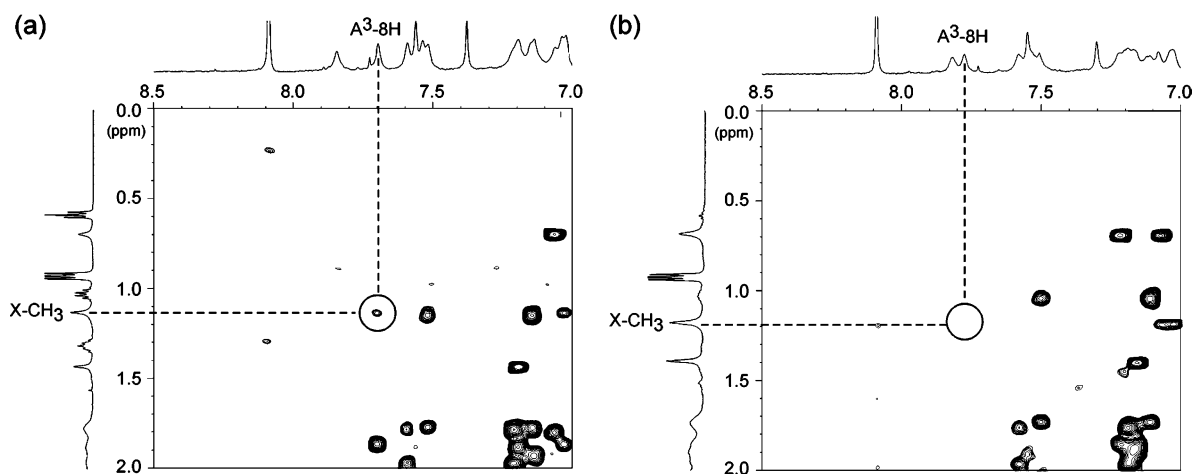


Figure 4. NOESY spectra (mixing time = 100 ms) of (a) *Azo-α/C* and (b) *Azo-β/C* at the regions of 1.0–2.0 ppm (X-CH₃) and 7.0–8.5 ppm (A³-8H) in D₂O at 280 K, in the presence of 0.2 M NaCl. A distinct NOE between X-CH₃ and A³-8H could be observed only for the *Azo-α/C* duplex, indicating that *Azo-α* corresponds to the *R*-configuration.

of the NOE. A total of 248 NOE distance restraints and 8 dihedral restraints were used for *Azo-α* and 274 NOE distance restraints and 6 dihedral restraints were used for *Azo-β* (Table 1). To determine the position of azobenzene, 53 and 70 restraints were used for *Azo-α/C* and *Azo-β/C*, respectively.⁸ The duplex structures were calculated using restrained molecular dynamics of a simulated annealing protocol (see Experimental Section for details). A total of 17 final structures for *Azo-α/C* (*R*-isomer as determined above) and 20 final structures for *Azo-β/C* (*S*-form) converged to a low total energy (see Figure 5a for *Azo-α/C* and 5b for *Azo-β/C*). The minimized averaged structures of both *Azo-α/C* and *Azo-β/C* are also shown in Figure 6. It can be seen that the *trans*-azobenzene intercalates between the base pairs of both diastereomers.⁹ As described in the previous section, the NMR analysis demonstrates that the *trans*-azobenzene intercalates between the adjacent base pairs of both diastereomers. The upfield chemical shift of the imino protons

Table 1. Statistical Restraints Used in the Structural Determination Protocol and Results of the Superpositions of the Converged Structures

	<i>Azo-α/C</i> ^a	<i>Azo-β/C</i> ^a
NOE distance restraints	248(53)	274(70) ^b
intraresidue	120(8)	138(12)
interresidue	128(45)	136(58)
dihedral restraints	8	6
hydrogen bonding distance restraints	16	16
base planarity restraints	6	6
heavy-atoms rms deviation (Å) ^c	1.44	1.14

^a Parentheses are the numbers of NOEs around the azobenzene used for the calculation. ^b 14 restraints (>5 Å) were added on the basis of the absence of NOE cross-peaks. ^c The averaged rmsd values between an average structure and converged structures were calculated. The converged structures did not contain an experimental distance violation of >0.2 Å or dihedral violation >10°.

of T¹⁰ and G⁴ is caused by stacking of azobenzene with A³-T¹⁰ and G⁴-C⁹ base pairs, because these imino protons are located near the axial position of the benzene ring B of the azobenzene moiety.

(9) Stereoviews of the duplexes from other angles are shown in Supporting Information Figure 2.

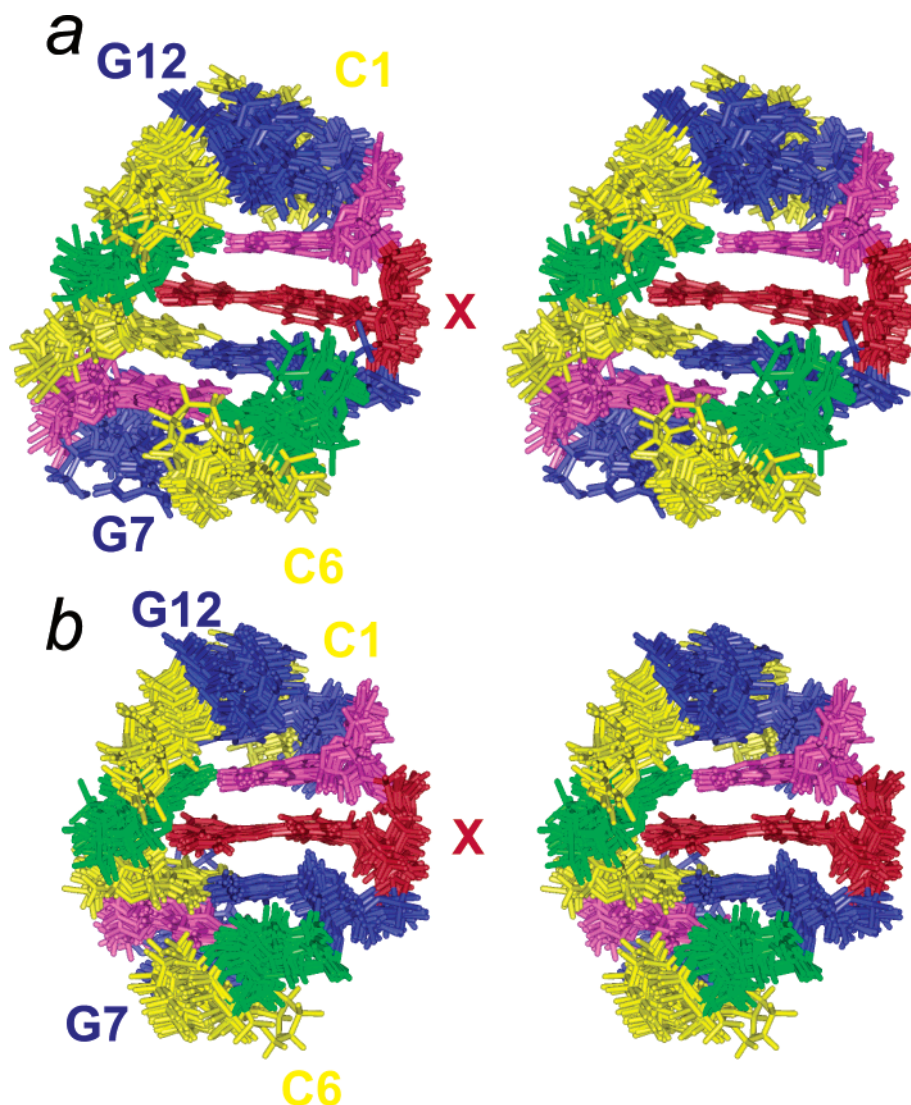


Figure 5. Stereoviews of the superposition of (a) the final 17 converged structures of **Azo- α /C** (*R*-configuration) and (b) 20 converged structures of **Azo- β /C** (*S*-configuration) duplexes. X, A, T, G, and C are colored in red, pink, green, blue, and yellow, respectively.

The structures of both duplexes are similar to each other, and only a small difference exists around the X residue. Some differences were found with regards to the stacked structures of the nucleobases around the X residue. The skew angle between A³–T¹⁰ and G⁴–C⁹ for **Azo- α /C** (*R*) was 35–36°, whereas for **Azo- β /C** (*S*) it was 30–31°. Because the skew angle of the natural duplex is 36° (note that the B-type helix has 10 base pairs per turn), intercalation of the *trans*-azobenzene on the linker with the *R*-configuration does not disturb the right-hand helix. On the contrary, the skew angle of the *S*-configuration was 5–6° smaller than that of the *R*-configuration, indicating that winding of the helix is slightly disturbed at the X residue.

3. Correlation between Melting Temperature and Configuration. The melting temperatures of the **Azo- α /C** (*R*) and **Azo- β /C** (*S*) duplexes in the *trans*-form were 37.1 and 32.7 °C, respectively, whereas the melting temperature for N/C, a native duplex without azobenzene, was only 30.1 °C under the conditions employed. This fact demonstrates that addition of azobenzene to a nonnatural linker does not destabilize the duplex.^{10,11} Rather, hydrophobic stacking between azobenzene and base pairs compensates for the disturbance of the natural

duplex by the nonnatural molecule on the linker so that the duplex is even more stable than the native 6-mer duplex.¹²

The melting temperature of **Azo- α /C** was higher than that of **Azo- β /C**, indicating that a linker with an *R*-configuration is preferable to that of an *S*-configuration for tethering azobenzene and stabilizing the duplex. This result correlates with the stacked structures of the nucleobases around the X residue. As described in the previous section, the skew angle between A³–T¹⁰ and G⁴–C⁹ for **Azo- β /C** (*S*-form) was 5–6° smaller than that of the **Azo- α /C** (*R*-form) or native duplex (see Figure 7). Because

- (10) The melting curves of both **Azo- α /C** and **Azo- β /C** duplexes either in the *trans*- or in the *cis*-form are presented in Supporting Information Figure 3.
- (11) Azobenzene was tethered on the chiral threoninol that has a structure similar to that of the present prochiral 2,2-bis(hydroxymethyl)propionic acid (Asanuma, H.; Takarada, T.; Yoshida, T.; Tamaru, D.; Liang, X.; Komiyama, M. *Angew. Chem., Int. Ed.* **2001**, *40*, 2671–2673). A similar dependence in melting temperature (*R*-form > *S*-form) for the chirality of the linker was observed. See Supporting Information Scheme 1 and Supporting Information Table 1.
- (12) In the present paper, the X residue is additionally incorporated into one strand of the full-matched natural double strands (7-mer/6-mer nonsymmetrical combination). However, placement of a nucleobase as the counterpart of the X residue, such as a 5'-CGAXGTC-3'/3'-GCTTCAG-5' (7-mer/7-mer symmetrical combination) duplex, destabilizes the duplex because intercalated *trans*-azobenzene directly faces the extra nucleobase and a mismatch-like structure is formed.

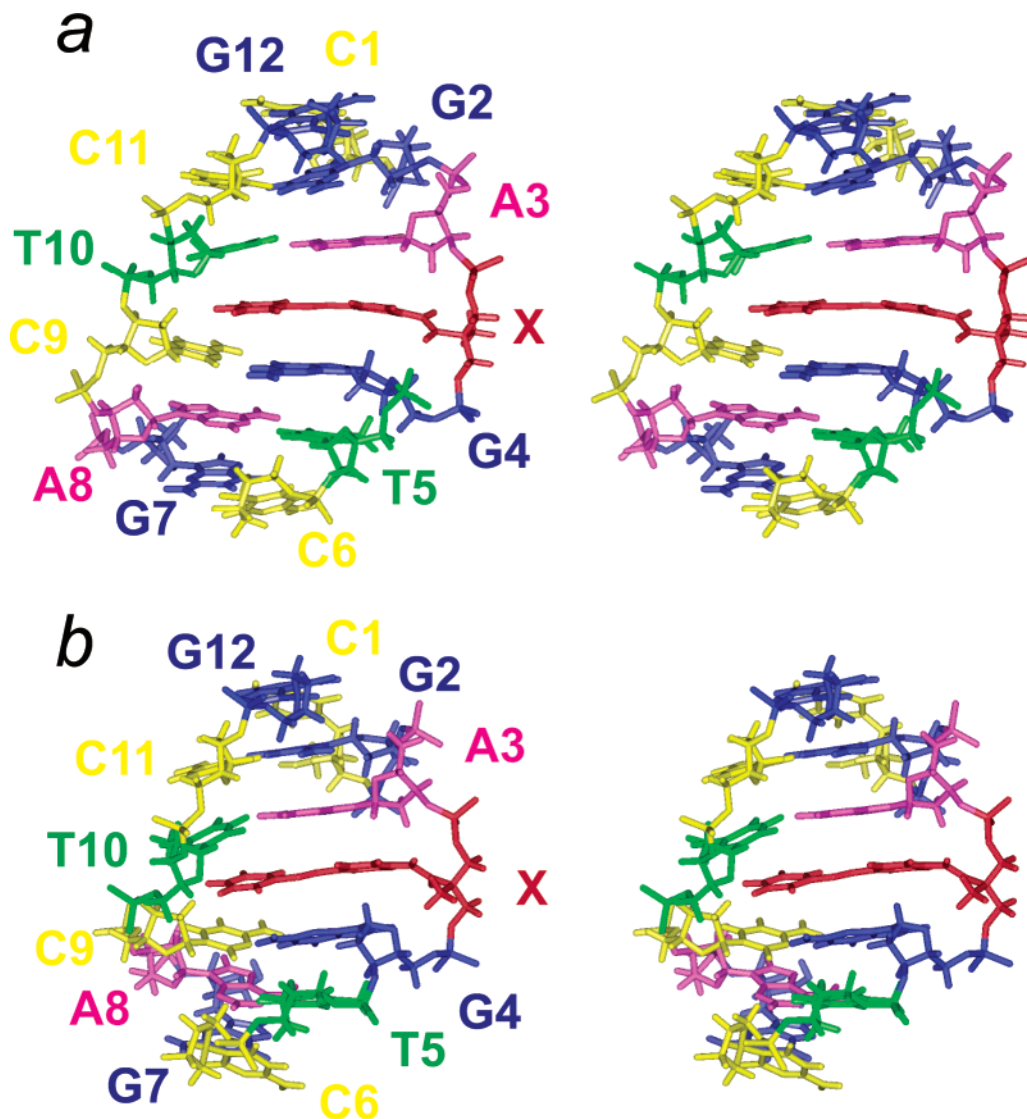


Figure 6. Minimized average structures (stereoviews) of (a) *Azo- α /C* (*R*) and (b) *Azo- β /C* (*S*) viewed from the side of the *trans*-azobenzene. The color scheme is the same as in Figure 5.

the *S*-form disturbs more seriously the right-hand helix in the formation of the duplex and induces greater strain than the *R*-form, the T_m of *Azo- α /C* is higher than that of *Azo- β /C*. These results demonstrate that the chirality of the linker tethering a functional molecule influences the stability of the duplex, although it may only cause subtle structural differences near the modification site. The chirality of the linker is an important factor to be considered when designing modified DNA.

Conclusion

The absolute configurations of two diastereomers of photoresponsive oligodeoxyribonucleotide, based on the chirality of the central carbon of the diol linker, have been assigned on the basis of NMR analysis. The diastereomer α (*Azo- α* , with a shorter retention time), which stabilizes the duplex more efficiently, was determined to be an *R*-configuration, and *Azo- β* was determined to be an *S*-configuration. For both diastereomers, the NMR-determined structures of the duplexes showed that *trans*-azobenzene intercalates between DNA base pairs. The hydrophobic and planar *trans*-azobenzene stabilizes the duplex by a stacking interaction. Differences in duplex stability between

the two diastereomers (*trans*-form) were based on the fact that the *S*-form causes more stress when forming the duplex than does the *R*-form due to disturbances in the right-hand helix. Thus, the chirality of the linker for tethering a functional moiety affects the properties of the modified DNA.

Experimental Section

A. Materials. The phosphoramidite monomers carrying azobenzene were synthesized as previously described.^{3,4} All conventional phosphoramidite monomers, CPG columns, reagents for DNA synthesis, and Poly-Pak cartridges were purchased from Glen Research Co. The digestion enzyme alkaline phosphatase (AP) was purchased from Wako Pure Chemical Industries Ltd., and snake venom phosphodiesterase (SV-PPDE) was purchased from Boehringer Mannheim.

B. Synthesis and Purification of the Oligonucleotides. All of the oligonucleotides used in this study were synthesized on an ABI DNA/RNA synthesizer model 394 by typical phosphoramidite chemistry. The synthesized oligonucleotides were purified by Poly-Pak cartridges and then by reversed-phase HPLC (Merck LiChrospher 100 RP-18(e) column). Modified DNAs tethering the X residue were synthesized from corresponding phosphoramidite monomers.^{3a,b,4} The two diastereomers (α and β in Scheme 1) based on the chirality of the central carbon atom in the linker were separated using the same reversed-phase HPLC

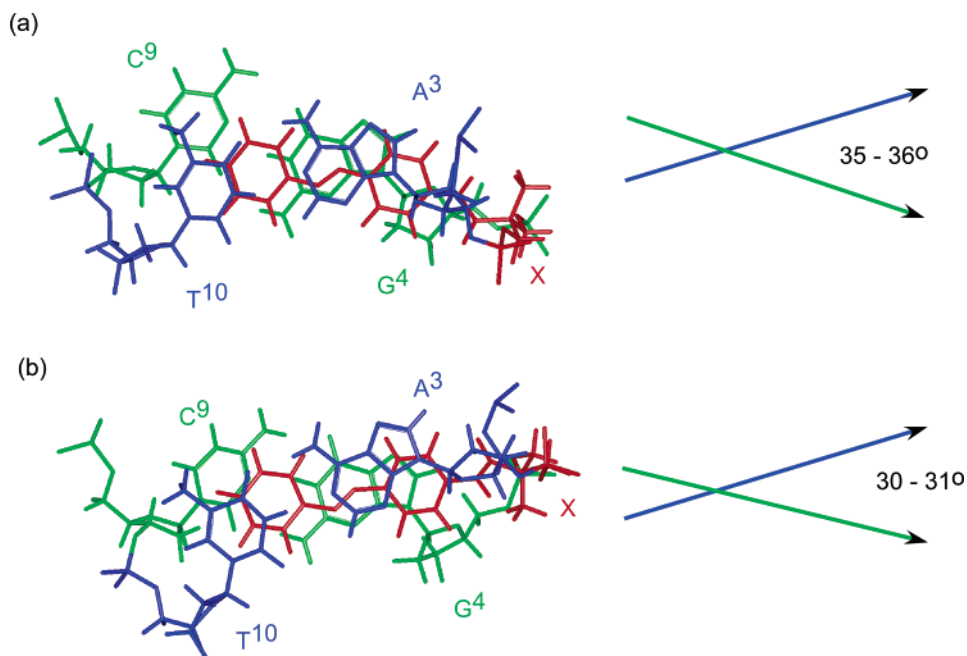


Figure 7. Stacked structures of (a) *Azo-α/C* (*R*) and (b) *Azo-β/C* (*S*) around the X residue as viewed along the helix axis. In the right-hand directions of A³–T¹⁰ (blue line) and G⁴–C⁹ (green line), base pairs in each diastereomer are represented as lines.

procedure. A linear acetonitrile/H₂O gradient (containing 50 mM ammonium formate) from 9.5/90.5 to 15/85 in 40 min was used as the elution agent. The difference in retention time between the two diastereomers was more than 2 min.

The concentration of oligonucleotides was determined by enzymatic digestion using alkaline phosphatase (AP) and snake venom phosphodiesterase (SV-PPDE). The error was controlled within 10%. The modified oligonucleotides used were further characterized by MALDI-TOFMS (negative mode).

Azo-α, obsd. 2165.7; **Azo-β**, obsd. 2165.5 (calcd. for [Azo-H⁺]: 2165.4).

C. NMR Experiments. NMR samples were prepared by dissolving three times lyophilized DNAs (modified and complementary DNA) to a concentration of 1.0 mM duplex in a H₂O/D₂O = 9/1 solution containing 10 mM sodium phosphate (pH 7.0). NaCl was added to a total sodium concentration of 200 mM. After NMR measurement in H₂O/D₂O, the samples were lyophilized again and dissolved in a D₂O solution.

NMR spectra were measured on a DRX-500 spectrometer (Bruker) at a probe temperature of 280 K. 2D NOESY (150 ms of mixing time) spectra¹³ in H₂O were recorded using the States-TPPI method¹⁴ and the jump-and-return water suppression scheme.^{15,16} FIDs (128 scans of each) of 2K data points in the *t*₂ domain were collected for 512 or 256 data points in the *t*₁ domain. Prior to Fourier transformation, the spectra were zero-filled to give final 2K × 1K data points after apodization with a $\pi/2$ -shifted squared sinebell function. 2D NOESY (50, 100, and 200 ms of mixing times), TOCSY (50 ms of mixing time),¹⁷ and DQF-COSY spectra¹⁸ in D₂O were recorded using the States-TPPI method without suppression of the H₂O signal. FIDs of the 2K data points in the *t*₂ domain were collected for the 1K data

points in the *t*₁ domain. The number of scans for NOESY, TOCSY, and DQF-COSY in D₂O were 48, 8, and 16, respectively. Prior to Fourier transformation, Gaussian window functions were applied to both dimensions.

D. Structural Restraints. NOE intensities obtained from 2D NOESY spectra in D₂O with a mixing time of 100 ms were interpreted as distances of very strong (0–3 Å), strong (0–4 Å), medium (0–5 Å), or weak (0–6 Å). The spectra were also measured with a mixing time of 50 ms, which confirmed that the distances calculated from the 50 ms data agreed with those from the 100 ms data within an error of 10%.¹⁹ Because the S/N of the 100 ms was much better than that of the 50 ms, we used 100 ms for the calculation. A few other interproton distances were obtained from the NOESY spectra in H₂O with a mixing time of 150 ms. Using cross-peaks corresponding to the fixed 2.4 Å deoxycytidine 5H–6H distance as internal references, we calculated interproton distances corresponding to each of the cross-peaks using the program Felix (Molecular Simulation, Inc.). For the distance restraints, upper and lower limits were defined as +2 and –1 Å calculated distances, respectively. For the β isomer, 14 restraints (>5 Å) were added to the distance restraints described above on the basis of the absence of NOE cross-peaks. To estimate the δ dihedral angle (C5'–C4'–C3'–O3'), the sugar pucker was analyzed using TOCSY and DQF-COSY spectra. A large ³J_{H1'–H2'} scalar coupling constant indicates a C2'-endo conformation ($\delta = 160 \pm 30^\circ$), whereas a small coupling constant corresponds to a C3'-endo conformation ($\delta = 85 \pm 30^\circ$).²⁰ In the case of **Azo-α**, residues 1–7, 11, and 12 were assigned as C2'-endo conformations, and 8–10 were assigned as C3'-endo conformations. In the case of **Azo-β**, residues 1–3, 5–7, 11, and 12 were assigned as C2'-endo conformations, and 4 and 9 were assigned as C3'-endo conformations. Hydrogen bonding restraints from Watson–Crick base pairs (three for a GC pair and two for an AT pair) were introduced as distance restraints between the proton and heavy atom (1.8–2.5 Å). The existence of hydrogen bonding for base pairs was judged from a significant downfield shift of the imino proton resonance and a slow rate of exchange with the solvent. For the residues at the ends of each strand (C¹, C⁶, G⁷, and G¹²), restraints on the typical B-form

(13) Jeener, J.; Meier, B. H.; Bachmann, P.; Ernst, R. R. *J. Chem. Phys.* **1979**, *71*, 4546–4553.

(14) Marion, D.; Ikura, M.; Tschudin, R.; Bax, A. *J. Magn. Reson.* **1989**, *85*, 393–399.

(15) Plateau, P.; Gueron, M. *J. Am. Chem. Soc.* **1982**, *104*, 7310–7311.

(16) We also measured NOESY spectra in H₂O by use of a 3-9-19 WATERGATE pulse sequence and confirmed that the sets of restraints for the calculation obtained from Jump and Return and WATERGATE were almost the same.

(17) Griesinger, C.; Otting, G.; Wüthrich, K.; Freeman, R. *J. Am. Chem. Soc.* **1988**, *110*, 7870–7872.

(18) Shaka, A. J.; Freeman, R. *J. Magn. Reson.* **1983**, *51*, 169–173.

(19) This result indicates that spin diffusion at 100 ms is still small and does not affect the distance interpretation. Note that the loose restraints were used for structural calculations.

(20) Allain, F. H.-T.; Varani, G. *J. Mol. Biol.* **1995**, *250*, 333–353.

DNA structure were introduced on the assumption that the X residue would not influence the structure of the ends of the DNA strands.

E. Structure Calculation. A set of 100 structures was calculated using a simulated annealing protocol with the InsightII/Discover package (Molecular Simulation, Inc.). The CVFF (consistent valence force field) was used as the force field.²¹ A total of 248 NOE distance restraints and 8 dihedral restraints were used for **Azo- α** , whereas 274 NOE distance restraints and 6 dihedral restraints were used for **Azo- β** . The force constants were 50 kcal mol⁻¹ Å⁻² for distance restraints and 50 kcal mol⁻¹ rad⁻² for dihedral restraints. At the beginning of the calculation, the atomic coordinates were randomized. Distance and dihedral restraints were gradually scaled to full value during 15 ps of molecular dynamics at 1000 K, while maintaining low value for interatomic repulsion, which was subsequently increased to full value during another 21 ps of dynamics. An additional 5 ps of dynamics was performed at 1000 K, and the temperature was gradually scaled to 300 K during 10 ps. A final minimization step was performed, which included a Lennard-Jones potential and no electrostatic terms. The 17 final structures for the **Azo- α /C** duplex and 20 final structures for the **Azo- β /C** duplex that had the lowest total and restraint violation energies were chosen.

F. Measurement of the Melting Temperature. The melting curve of the duplex was obtained by measuring the change of absorbance versus temperature at 260 nm (JASCO model V-530 spectrophotometer involving a programmed temperature-controller). The buffer solution was composed of 10 mM sodium phosphate (pH 7.0) and 1 M NaCl,

and the concentration of DNA was 50 μ M. The melting temperature (T_m) was determined from the maximum in the first derivative of the melting curve. Heating (from low to high temperature) and cooling (from high to low temperature) curves were both measured, and the T_m of these methods coincided with each other within ± 1.0 °C. The T_m values reported are an average of 2–4 experiments.

Acknowledgment. This work was financially supported by Precursory Research for Embryonic Science and Technology (PRESTO), Japan Science and Technology Agency (JST). Partial supports by The Iwatani Naoji Foundation, Atsumi International Scholarship Foundation (for X.L.), The Mitsubishi Foundation (for H.A.), and a Grant-in-Aid for Scientific Research from the Ministry of Education, Science, and Culture, Japan, are also acknowledged. This work was also supported, in part, by a “Research for the Future” Program (JSPS-RFTF97L00503) from the Japan Society for the Promotion of Science.

Supporting Information Available: Figure 1 (NOEs from the protons on the azobenzene), Figure 2 (stereoviews of the duplexes from other angle), Figure 3 (melting curves of the **Azo- α /C** and **Azo- β /C** duplexes), Scheme 1 (absolute configuration of each diastereomer), and Table 1 (correlation between the absolute configuration of the linker and melting temperatures) (PDF). This material is available free of charge via the Internet at <http://pubs.acs.org>.

(21) Dauber-Osguthorpe, P.; Roberts, V. A.; Osguthorpe, D. J.; Wolff, J.; Genest, M.; Hagler, A. T. *Proteins* **1988**, *4*, 31–47.

JA037248J